



Cite this: *Green Chem.*, 2015, **17**, 2271

## Recyclable hydrotalcite catalysts for alcohol imination *via* acceptorless dehydrogenation†

John Bain, Philip Cho and Adelina Voutchkova-Kostal\*

Here we report that hydrotalcite-like materials (HTs) are active heterogeneous catalysts for alcohol imination, which proceeds through acceptorless alcohol dehydrogenation. The catalytic activity of a series of Mg–Al hydrotalcites doped with Fe<sup>3+</sup>, Zn<sup>2+</sup>, Ni<sup>2+</sup>, Cr<sup>3+</sup> and Cu<sup>2+</sup> is dependent on their composition, and Fe : Mg : Al HT yields up to 92% imine under mild conditions. Impregnation of Fe : Mg : Al HT with Pd<sup>0</sup> resulted in an enhancement of activity for acceptorless dehydrogenation, but a decrease in the isolated yield of imine in a loading-dependent manner. This is attributed to the Pd loading-dependent retention of imine and aldehyde on the catalysts. The substrate scope for alcohol imination and recyclability of the catalysts is discussed.

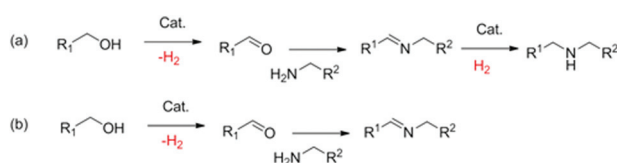
Received 9th February 2015,  
Accepted 4th March 2015

DOI: 10.1039/c5gc00312a

www.rsc.org/greenchem

### Introduction

Imines are highly versatile intermediates for the stereoselective synthesis of amines and N-heterocycles.<sup>1</sup> Synthetic routes to imines that utilize readily available starting materials, such as alcohols, are typically more atom-economical than conventional routes requiring carbonyl compounds. Alcohol imination reactions can proceed through alcohol oxidation to the corresponding ketone or aldehyde, followed by condensation with the amine. Amination catalysts typically proceed through alcohol dehydrogenation, amine condensation and imine hydrogenation (Scheme 1a).<sup>2–10</sup> Alcohol imination can proceed through a similar route lacking the hydrogenation step (Scheme 1b). Although a number of highly active catalysts have been reported for alcohol amination,<sup>4,8,10–18</sup> catalytic systems that yield the imine are rare and offer the advantageous possibility of further imine functionalization.<sup>17,19–23</sup>



**Scheme 1** Catalytic alcohol (a) amination and (b) imination *via* dehydrogenation.

Department of Chemistry, The George Washington University, Washington, DC, USA.  
E-mail: avoutchkova@email.gwu.edu; Fax: +202-994-5873; Tel: +202-994-6121

† Electronic supplementary information (ESI) available. See DOI: 10.1039/c5gc00312a

Hydrotalcites (HTs) are layered double hydroxides (LDHs)<sup>24</sup> with the general formula  $[M^{2+}_{1-x}M^{3+}_x(OH)_2]^{x+}(A^{n-})_{x/n} \cdot mH_2O$ , where A<sup>−</sup> represents anions (e.g. CO<sub>3</sub><sup>2−</sup>, OH<sup>−</sup>, Cl<sup>−</sup>, NO<sub>3</sub><sup>2−</sup>, SO<sub>4</sub><sup>2−</sup> etc.) and M<sup>2+</sup> and M<sup>3+</sup> are compatible alkali earth and transition metal ions (e.g. Fe<sup>3+</sup>, Zn<sup>2+</sup>, Ni<sup>2+</sup>, Cr<sup>3+</sup>, Cu<sup>2+</sup>, Co<sup>2+</sup> etc.). Although variation in the composition does not impact the brucite-like structure,<sup>24</sup> it does affect the acid/base,<sup>25–28</sup> redox,<sup>28</sup> and catalytic properties of these materials.<sup>25,29–33</sup> Particle size and morphology can also be varied by modifying the synthetic protocol.<sup>34–37</sup> In addition, the LDH structure itself can be semi-reversibly transformed to that of a mixed metal oxide (MMO) by calcination at ~450 °C.<sup>38,39</sup> MMOs outperform the corresponding LDHs in a number of catalytic applications, as they are significantly more basic and resistant to sintering.<sup>38</sup> Rehydration of MMOs causes incomplete reversion to a more basic LDH phase *via* a “memory effect”.<sup>33,40</sup> Thus, by controlling composition, synthetic protocol and post-synthetic treatment a palette of synthetic HTs can be accessed with comparable structures, but substantial differences in catalytic activities. This allows optimization of the catalytic activity by varying the HT composition.<sup>38</sup>

HTs are increasingly used as heterogeneous catalysts for a number of base-assisted solution-phase reactions that operate under mild conditions. Examples include aldol condensations,<sup>41–43</sup> Claisen–Schmidt condensations,<sup>44</sup> acylation of phenols, amines and thiols,<sup>45</sup> epoxidations,<sup>46</sup> transesterifications,<sup>47</sup> and N-arylation of amines.<sup>48</sup> HTs have also been reported as catalysts for alcohol oxidation that takes place under mild conditions: Sakthivel *et al.* have recently reported a Co/Al hydrotalcite system;<sup>49</sup> and Choudary<sup>50</sup> and Takehira<sup>51</sup> have reported a Ni/Mg/Al hydrotalcite system for alcohol oxidation using molecular oxygen. However, acceptorless

alcohol dehydrogenation is a more attractive approach due to the higher atom economy and generation of hydrogen gas. The catalytic activity of Mg–Al HTs for acceptorless alcohol dehydrogenation is only reported under high temperature and pressure conditions (533 K, 100 kPa) in the gas phase.<sup>52</sup> Alcohol imination using HTs has not been reported to the best of our knowledge, but there is one example of alcohol amination using a Cu/Al hydrotalcite, which likely proceeds through alcohol dehydrogenation.<sup>53</sup>

In addition to the interest in HTs as heterogeneous catalysts, they are also increasingly used as “inert” supports for other catalysts. Examples include supported Rh,<sup>54</sup> V,<sup>55</sup> and Ru<sup>56</sup> oxides and nanoparticles (n.p.) of Ag, Pd,<sup>57</sup> Au,<sup>58</sup> Cu,<sup>59</sup> Ru,<sup>60</sup> Rh,<sup>61</sup> and Ni.<sup>62</sup> Nanoparticles of Ag, Pd, and Cu supported on Mg–Al HTs are reported as active catalysts for acceptorless alcohol dehydrogenation under mild conditions. Although these reports note that the HT support is critical for catalytic activity,<sup>59,60,63–66</sup> they do not attribute inherent catalytic activity for dehydrogenation to the HT itself.<sup>51,60,67,68</sup>

While exploring the catalytic activity of HT-supported Pd n.p. for alcohol imination, we observed that some HTs exhibit inherent catalytic activity for alcohol dehydrogenation and imination. Here we report the optimization of a modified hydrotalcite that can act as an efficient, cheap and recyclable heterogeneous catalyst for alcohol imination under mild conditions. We show that supported Pd<sup>0</sup> can enhance activity for dehydrogenation, but actually retard activity for imination.

## Results and discussion

Six modified Mg–Al hydrotalcites (HTs) were synthesized with the addition of the first row transition metal ions. The first row metals were selected due to their relative abundance in comparison with the second and third row transition metals, and the compatibility of their ionic radii for incorporation into the HT lattice. The metal ions selected (Cr<sup>3+</sup>, Fe<sup>3+</sup>, Ni<sup>2+</sup>, Cu<sup>2+</sup> and Zn<sup>2+</sup>) provide a range of acid–base properties, hydridic/protic behaviour and redox potentials. HTs 1–6 were synthesized by co-precipitation and aging of the corresponding transition metal nitrate salt with Mg(NO<sub>3</sub>)<sub>2</sub>·6H<sub>2</sub>O and Al(NO<sub>3</sub>)<sub>3</sub>·9H<sub>2</sub>O. Table 1 shows the elemental composition, powder X-ray diffraction (PXRD) parameters and BET surface areas of the resulting HTs 1–6. The PXRD and BET surface area parameters are consistent with literature values (ESI Table S1†).

Powder X-ray diffraction (PXRD) patterns confirmed the phase, phase transition, crystallinity and lattice parameters of the HTs, as well as Pd-impregnated HTs (Pd/HTs) discussed in a later part of the manuscript. Exemplary PXRD patterns are shown in Fig. 1. The PXRD patterns of all six HTs (shown in ESI Fig. S1†) were consistent with the pure HT phase, characterized by sharp symmetric reflections (003 and 006) and broad asymmetric reflections.<sup>24</sup> The lattice parameters *a* and *c* (average cation–cation distance and three

**Table 1** Characterization data of hydrotalcites (HTs) 1–6

Cat.	M <sup>a</sup>	% Elemental composition (FAAS)			PXRD crystallographic parameters <sup>b</sup>			BET S.A. (m <sup>2</sup> g <sup>-1</sup> )
		Mg	Al	M <sup>a</sup>	<i>a</i> (Å)	<i>c</i> (Å)	<i>L</i> (nm)	
HT1	—	28.3	9.28	—	3.001	23.348	16.9	63
HT2	Zn	20.9	6.95	29.0	3.005	23.186	10.0	128
HT3	Cu	21.9	8.54	13.2	2.992	22.986	15.0	30
HT4	Fe	29.4	3.05	11.4	3.082	23.145	20.0	73
HT5	Ni	25.0	10.2	14.0 <sup>c</sup>	2.998	23.346	12.9	64
HT6	Cr	25.2	3.36	10.1 <sup>c</sup>	3.020	23.067	11.9	5

<sup>a</sup> The third metal added to the Mg/Al HT. <sup>b</sup> *a*, the average cation–cation distance; *c*, three times the distance from the centre of one brucite-like layer to the next layer; *L*, the average crystallite size (lower bound, calculated using Scherrer's formula).<sup>69</sup> <sup>c</sup> Values obtained by EDX.

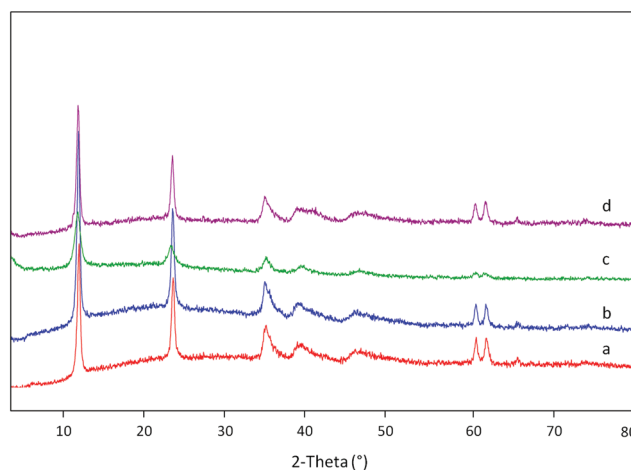


**Fig. 1** PXRD patterns of (a) HT4, (b) 0.02% Pd/HT4, (c) 1% Pd/HT4, and (d) 5% Pd/HT4.

times the distance from the centre of one brucite-like layer to the next, respectively) were all within 0.015 Å and 0.92 Å ranges respectively, suggesting only minute differences in the lattice structures of the HTs. The variation in composition is reflected in an evident variability in the BET surface areas of HTs 1–6 (5–128 m<sup>2</sup> g<sup>-1</sup>). This is due to small differences in the synthetic protocols for the respective HTs, differences in the rates of co-precipitation and porosity of the resulting HT. The BET surface area of the HT6, which contains 10.1% Cr<sup>3+</sup>, is reproducible but anomalously low due to very low porosity relative to the other HTs. PXRD and FT-IR characterization of HT6 was consistent with HT as the only phase.

HTs 1–6 were also characterized by FT-IR. Fig. 2 shows exemplary FT-IR spectra of HT4 and the series of Pd/HT4 with varying loadings of Pd, while spectra for HTs 1–6 are shown in ESI Fig. S2.† Carbonate anions were detected in all HTs and Pd/HTs, as indicated by the ν<sub>C=O</sub> at 1350–1370 cm<sup>-1</sup>. Broad bands arising from bending vibrations of interlayer water are

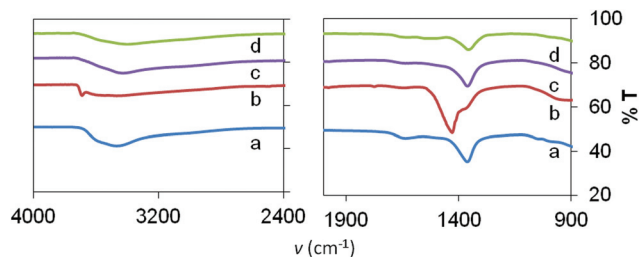


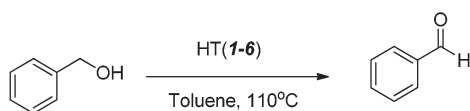
Fig. 2 FT-IR spectra of (a) HT4, (b) 0.02% Pd/HT4, (c) 1% Pd/HT4, and (d) 5% Pd/HT4.

observed between  $\sim 1400$  and  $1700\text{ cm}^{-1}$ . Since the symmetry of the interlayer water molecules is affected by composition, some HTs show additional broad bands in that region. Nitrate anions were not detected (no sharp peak at  $1376\text{ cm}^{-1}$ ),<sup>70</sup> indicating that nitrate salts of the starting materials had been washed out of the lattice.

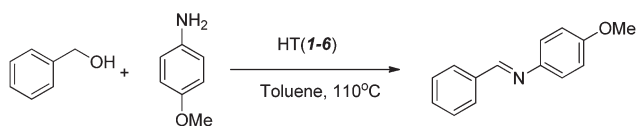
### Catalytic activity of hydrotalcites for alcohol dehydrogenation and imination

The catalytic activity of HTs 1–6 towards alcohol dehydrogenation (Scheme 2) and imination (Scheme 3) of benzyl alcohol in the absence of a base is summarized in Fig. 3.

The yields of aldehyde resulting from alcohol dehydrogenation are lower than the yields of imine, which implies that the amine improves dehydrogenation yield by drawing the equilibrium towards products *via* condensation with the aldehyde. A general correlation between the activities for both reactions was observed, consistent with imination occurring *via* dehydrogenation. The molar ratio of  $\text{H}_2$  to benzaldehyde was within experimental error of being stoichiometric (89 : 100) in the dehydrogenation of benzyl alcohol, thus indicating that  $\text{H}_2$  is generated quantitatively during the reaction. A clear difference in catalytic activity was observed among the six HTs. In contrast to the negligible yield of the imine afforded by HT6 (Cr : Mg : Al), HT4 (Fe : Mg : Al) afforded 85% imination



Scheme 2 Catalyst screening for alcohol dehydrogenation.



Scheme 3 Catalyst screening for alcohol imination.

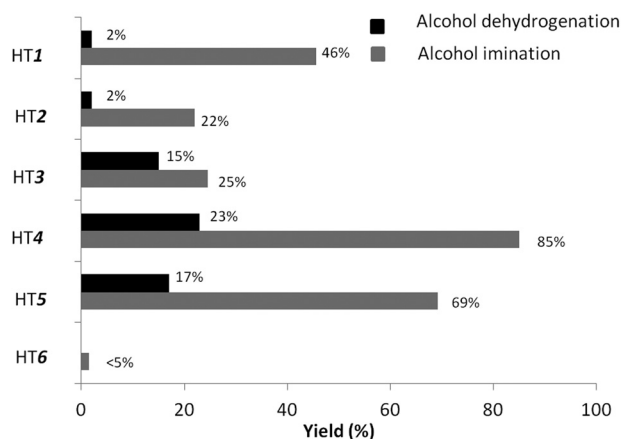
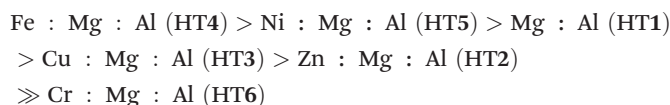


Fig. 3 Percent yields of benzaldehyde and 4-methoxy-*N*-(phenylmethylene)benzenamine from reactions in Schemes 2 and 3. Alcohol dehydrogenation reaction conditions: 0.24 mmol of benzyl alcohol, 0.100 g of catalyst, 3 mL toluene, 110 °C, 48 h. Yields were determined from GC-FID with an internal standard (trimethoxybenzene). Alcohol iminations were carried out under identical conditions, with the addition of 0.29 mmol *p*-anisidine.

product under the screening conditions. The observed relative catalytic activity of the HTs for imination is as follows:



Optimization of solvents for imination reactions increased the yield afforded by HT4 to 92% when xylenes were used as solvents. The reaction proceeds without the need for an external base, and addition of  $\text{K}_2\text{CO}_3$  did not improve the yield. Although the aniline present is itself a homogeneous base, results from alcohol dehydrogenation experiments confirm that no external base is necessary for dehydrogenation. In contrast, homogeneous catalysts for similar processes do not generally operate efficiently without an external base.<sup>17</sup>

Given the similar lattice structures of the six HTs, these differences in activity are likely due to the respective acid–base properties, redox properties, and catalytic surface areas. Although differences in surface areas cannot account for the variation in catalytic activity, the lack of activity for HT6 is likely associated with its anomalously low surface area and the lack of porosity that is apparent from the gas adsorption isotherms. The differences in acid–base and redox properties are currently under investigation, and likely have a predominant influence on catalytic activity. Preliminary microcalorimetry results<sup>76</sup> that probe the heats of adsorption of  $\text{CO}_2$  showed HT4 to have intermediate basicity among the series, which implies that there is likely an optimal basicity associated with the highest catalytic activity. It should also be noted that trends from microcalorimetric studies are impacted by the surface area, volume of pore or diameter of pore. The latter three are not consistent across HTs 1–6, as indicated in

**Table 2** Percent yields of (a) 4-methoxy-*N*-(phenylmethylene)benzenamine and (b) benzaldehyde from imination or dehydrogenation of benzyl alcohol facilitated by HT4 with different thermal treatments (HT4: freshly prepared; HT4<sub>calc</sub>: calcined at 450 °C and HT4<sub>reh</sub>: calcined at 450 °C and then rehydrated)

	HT4	HT4 <sub>calc</sub>	HT4 <sub>reh</sub>
Dehydrogenation (Scheme 2) <sup>a</sup>	23	37	8
Imination (Scheme 3) <sup>a</sup>	92	77	38

<sup>a</sup> Conditions as described in Fig. 3.

Table 1, so further research efforts are focused on optimizing the synthetic protocols so as to make surface areas consistent. This will allow us to explicitly probe the effect of basicity.

Since the basicity of HTs can be enhanced semi-reversibly by calcination<sup>38,39</sup> and by calcination–rehydration,<sup>33,40</sup> we also probed the catalytic activity after calcination of HT4 at 450 °C and after calcination–rehydration. This treatment afforded HT4<sub>calc</sub> and HT4<sub>reh</sub> respectively. Under the optimized conditions both were less active for imination than the HT4, although HT4<sub>calc</sub> showed higher dehydrogenation activity (Table 2).

We initially hypothesized that the enhanced basicity of HT4<sub>calc</sub> and HT4<sub>reh</sub> would translate into higher activity for dehydrogenation, as the basic sites are implicated in deprotonation of the alcohol and β-hydride elimination. Indeed we observe a higher dehydrogenation yield with HT4<sub>calc</sub>. However, HT4<sub>calc</sub> and HT4<sub>reh</sub> both afford lower imination yields than HT4. To test whether this decrease in yield is due to the adsorption of aldehyde and/or imine to the HT, we monitored the concentration of free aldehyde and imine respectively when each was reacted with HT4, HT4<sub>calc</sub> and HT4<sub>reh</sub> respectively. We found that HT4<sub>calc</sub> retains 53% and 41% after 24 h of reaction. Under the same conditions HT4<sub>reh</sub> retains 28% of the imine and 35% of the aldehyde respectively. Given that HT4 retains smaller fractions of aldehyde and imine, the lower yields of aldehyde (for HT4<sub>reh</sub>) and imine (for HT4<sub>calc</sub> and HT4<sub>reh</sub>) are likely due to the adsorption of the products on the catalyst. Extensive washing of the catalyst did not release additional products.

### Catalytic activity of Pd<sup>0</sup> on Fe–Mg–Al hydrotalcite for alcohol dehydrogenation and imination

Given that HT4 was the most active HT catalyst for both dehydrogenation and imination, we expected that immobilization of small quantities of Pd(0) on this support would boost the catalytic activity. This is consistent with literature reports that document alcohol dehydrogenation facilitated by immobilized Pd on Mg/Al HT.<sup>60,63,71</sup> We thus synthesized and characterized three Pd/HT4 catalysts with different Pd loadings (Table 3). The presence of Pd was confirmed by AAS and TEM/EDX. TEM images did not show distinct Pd nanoparticles, suggesting that the Pd phase is highly dispersed (ESI Fig. S3†). The PXRD parameters and the elemental composition of palladium on HT4

**Table 3** Characterization data of Pd/HT4 catalysts (Pd/HT4): Pd composition (determined from atomic absorption spectroscopy) and PXRD crystallographic parameters (*a*, *c* and *L*)

Catalyst	% Pd (AAS)	PXRD crystallographic parameters <sup>a</sup>		
		<i>a</i> (Å)	<i>c</i> (Å)	<i>L</i> (nm)
0.02% Pd/HT4	0.020	3.097	23.640	16.9
1% Pd/HT4	1.050	3.052	22.711	12.6
5% Pd/HT4	4.875	3.055	23.226	12.0

<sup>a</sup> *a*, the average cation–cation distance; *c*, three times the distance from the center of one brucite-like layer to the next layer; *L*, the average crystallite size (lower bound, calculated using Scherrer's formula).<sup>69</sup>

are shown in Table 3. PXRD patterns showed no detectable Pd phase and only minor variations from the crystallographic parameters of HT4 (Fig. 1). No detectable change in the HT4 interlayer spacing by PXRD is consistent with a highly dispersed Pd phase.<sup>72,73</sup> The FT-IR spectra of Pd/HT4 show broadening of the O–H ( $\nu_{\text{O-H}}$  at 3000–3600 cm<sup>-1</sup>) bands, suggesting a greater degree of hydrogen bonding in the surface and/or interlayer water. Small shifts in the carbonate band ( $\nu_{\text{C=O}}$  at ~1400 cm<sup>-1</sup>) and stretches related to interlayer water at 1560–1700 cm<sup>-1</sup> likely result from the changes in the symmetry of interlayer water molecules.

The catalytic activity of the Pd/HT4 as it relates to the Pd loading is illustrated in Fig. 4 and Table 4.

The aldehyde yields isolated from alcohol dehydrogenation (Scheme 2) were dependent on the Pd<sup>0</sup> loading, with the highest yield (85%) obtained with the 1% Pd/HT4 catalyst after 2 h (0.039 mol% Pd vs. alcohol), dropping to 65% when Pd<sup>0</sup> loading on HT4 was increased to ~5% (0.191 mol% Pd). The trend is illustrated in Fig. 4. The lower yields with 5% Pd/HT4 are likely due to the agglomeration of Pd, as confirmed by TEM. In contrast, in the 1% Pd/HT4 catalyst no distinct nanoparticles were observed by TEM, suggesting a more dispersed Pd phase. The fact that Pd impregnation enhances the aldehyde yield suggests that HT4-supported Pd<sup>0</sup> is more

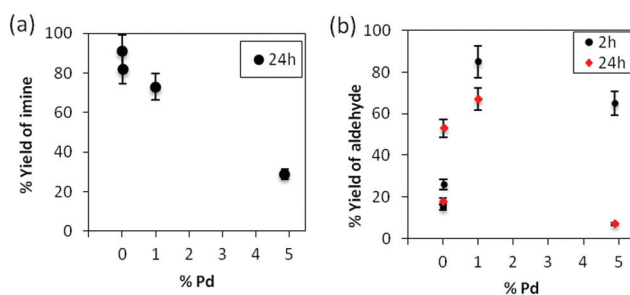


**Fig. 4** Percent yields of (a) imine from Scheme 3 and (b) benzaldehyde from Scheme 2 versus % Pd loading on HT4. Reaction conditions: 0.24 mmol of benzylalcohol, mol% Pd as shown in Table 4, 3 mL toluene, 110 °C, 24 h. Yields were determined from GC-FID using trimethoxybenzene as an internal standard. Error bars designate estimated standard error arising from measurement error and multiple runs.

**Table 4** Percent yields of benzaldehyde and 4-methoxy-*N*-(phenylmethylene)benzenamine from reactions in Schemes 2 and 3

Catalyst	mol% Pd <sup>a</sup>	%Yield		
		Imine, 24 h <sup>b</sup>	Aldehyde, 2 h <sup>b</sup>	Aldehyde, 24 h <sup>b</sup>
HT4	0	85	15	23
0.02% Pd/HT4	0.001	82	26	53
1% Pd/HT4	0.039	73	85	67
5% Pd/HT4	0.191	29	65	7

<sup>a</sup> mol% Pd relative to benzyl alcohol. <sup>b</sup> Conditions as described in Fig. 3.

catalytically active for dehydrogenation than the support (HT4) alone. Interestingly, the aldehyde yields at 2 h of reaction were higher than those at 24 h (Table 4). The decrease was especially noticeable for reactions with 5% Pd/HT4, where the aldehyde yield decreased from 65% (2 h) to 7% (24 h). Since the recovered unreacted alcohol can account for mass balance, we hypothesized that this was due to aldehyde being adsorbed to the catalyst. Thus we quantitated the fraction of free aldehyde in control reactions, where the alcohol was replaced by aldehyde under identical reaction conditions. We found that while the loss of aldehyde with 0.02% Pd/HT4 is negligible, with 1% Pd/HT4 we lose up to 30% of the aldehyde in 2 h, while with the 5% Pd/HT4 that number increases to 44%, and these quantities increase with time. These results suggest that the lower yield of aldehyde after 24 h *vs.* after 2 h could be attributed to adsorption of the aldehyde to Pd/HT4. The quantity of aldehyde bound is dependent on the loading of Pd on the HT (and the mol% Pd).

The yield of imine from the reaction in Scheme 3 decreases almost linearly with increasing Pd loading (Table 4 and Fig. 4). Thus, HT4 is the most active catalyst (85% yield), but just 0.02% Pd loading on the catalyst (0.001 mol% Pd) causes a decrease in the isolated yield to 82%. We proposed that this trend is due to the retention of aldehyde, amine and/or imine by the catalyst, and this retention is dependent on the Pd loading. Free aniline was observed in the reactions and is accounted for by mass balance, and a Pd loading-dependent retention of aldehyde has already been established in the previously described experiment. The amount of imine retained was almost equal for HT4 and 1% Pd/HT4 (22–26%) but higher for 5% Pd/HT4 (43%). Strong binding of Pd to imines is not surprising given the homogeneous catalysis literature. Despite the fact that these results are consistent with the hypothesis, we have not excluded the possibility that there may be more complex reasons that drive the difference in imine yields obtained from Pd/HT4 catalysts and HT4, such as the effect of immobilized Pd on the number and strength of acid–base sites on the HT4. Microcalorimetric studies are underway to investigate the effect of Pd on the acid–base properties of HTs.

Although we typically report TON and TOF when describing a new catalyst, in this case these metrics cannot be meaning-

fully established, as the active sites on these catalysts have not yet been identified or quantified. That is to say, we cannot assume that the Pd species are the only active catalyst, as our data clearly show the HT4 itself is catalytically active for alcohol dehydrogenation. The investigation of the mechanism and active sites of these catalysts is the topic of ongoing studies, which include an in-depth study of the electronic support interactions between Pd and HT4.<sup>39,74</sup>

### Substrate scope for imination

The alcohol substrate scope for imination using HT4 under optimized reaction conditions is shown in Table 5. Benzylic alcohols generally showed good to excellent yields. The reaction is favoured by electron-donating substituents of the benzene ring, such as methoxy (entries 1 and 3: 97% and 89%) and disfavoured by strongly electron-withdrawing nitro groups, which reduce the yield to 75% (entry 5). Benzyl alcohol itself also gave excellent yields of imine (92%, entry 2). Interestingly, a low yield was obtained with 4-(hydroxymethyl)phenol (15%, entry 7) despite the electron-donating –OH group. Phenol could be deprotonated by the basic catalyst to form the corresponding phenoxide, which could competitively inhibit activation of the benzylic alcohol on the HT4. The resulting phenoxide might also intercalate and become immobilized in the HT interlayers, resulting in decreased product yield. The extension of the benzylic alcohol by one methylene group to phenethyl alcohol reduces the yield to 32%, indicating that this mild catalytic system is selective for activated alcohols. Primary and secondary aliphatic alcohols show no reaction under these conditions (entries 8 and 9). It is notable that under the conditions reported by Uemura *et al.*, Pd/HT systems do not show a similar selectivity for alcohol dehydrogenation,<sup>67,68,75</sup> and are reactive for aliphatic alcohols.

The amine substrate scope using optimized reaction conditions and HT4 is shown in Table 6. The yields observed with anilines were strongly influenced by the ring substituents. Anilines with electron donating groups, such as methoxy (entry 1), afforded high yields, while those with strongly electron-withdrawing nitro groups resulted in lower isolated yields (entry 2). These electronic effects of ring substitution mirror the trends observed in the alcohol substrate series and are reflective of the more nucleophilic anilines being more reactive. The yields obtained with primary aliphatic amines were reasonably good (43–57%, entries 3–5). The results are not reflective of a direct trend with amine basicity, likely because more basic amines adsorb on the HT more strongly and are not available to condense with the aldehydes.

### Catalyst recycling

The ability to reuse the heterogeneous catalyst and identify compositional and morphological changes post-catalysis is critical for synthetic applications. Since in a few instances we observed conversions that were greater than yields, it was prudent to characterize the used catalysts, ensure that the organic material is not retained and check whether activity is

Table 5 Alcohol substrate scope for HT4-catalyzed alcohol imination

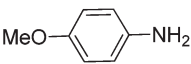
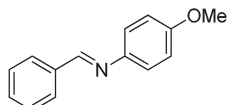
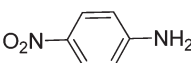
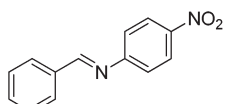
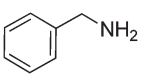
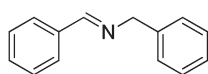
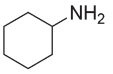
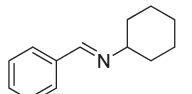
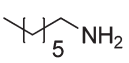
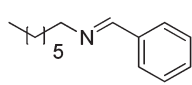
Entry	Alcohol substrate	Product	Yield (%)	Conversion (%)
1 <sup>a</sup>			97	99
2 <sup>a</sup>			92	97
3 <sup>a</sup>			89	100
4 <sup>a</sup>			84	98
5 <sup>a</sup>			75	93
6 <sup>a</sup>			32	90
7 <sup>a,b</sup>			15	54
8 <sup>b</sup>		—	NR	94
9 <sup>b</sup>		—	NR	73

<sup>a</sup> Reaction conditions: 0.24 mmol alcohol, 0.60 mmol *p*-anisidine, 100 mg catalyst, 3 mL xylenes, 110 °C, 24 h. <sup>b</sup> 200 mg catalyst.

retained in multiple use cycles. Indeed, TGA of the used and unwashed catalyst (HT4) from the reaction in entry 1 in Table 5 showed a new mass loss at 185 °C. We find that aqueous potassium carbonate provides the necessary abundance of carbonate ions to reform the active catalyst quickly during the wash and remove adsorbed substrates. The reformation to a LDH phase was confirmed by FT-IR and PXRD (Fig. 6), while the loss of residual organics was confirmed by TGA. The PXRD pattern of the used catalyst prior to wash

shows new reflections at 8.23° and 31.5° ( $2\theta$ ), which could not be readily attributed to an identifiable phase, but disappeared after aqueous  $K_2CO_3$  wash. It is notable that the PXRD patterns of the unwashed catalyst do not show any shift of the 003 reflection, which indicates that there is no change in interlayer spacing that would likely result from intercalation of substrates or products. The FT-IR spectra were consistent with the PXRD data – the unwashed catalyst shows several new IR stretches in the hydroxyl and carbonyl regions that are elimi-

**Table 6** Amine substrate scope for HT4-catalyzed alcohol imination

Entry	Amine substrate	Product	Yield (%)
<chem>c1ccc(cc1)CO + RR'NH &gt;&gt;[HT4, xylenes, 110°C] c1ccc(cc1)C=NRR'</chem>			
1 <sup>a</sup>			97
2 <sup>a</sup>			20
3 <sup>a</sup>			43
4 <sup>a</sup>			57
5 <sup>b</sup>			57

<sup>a</sup> Reaction conditions: 0.24 mmol benzyl alcohol, 0.29 mmol amine, 100 mg catalyst, 3 mL xylenes, 110 °C, 24 h. <sup>b</sup> 0.6 mmol amine.

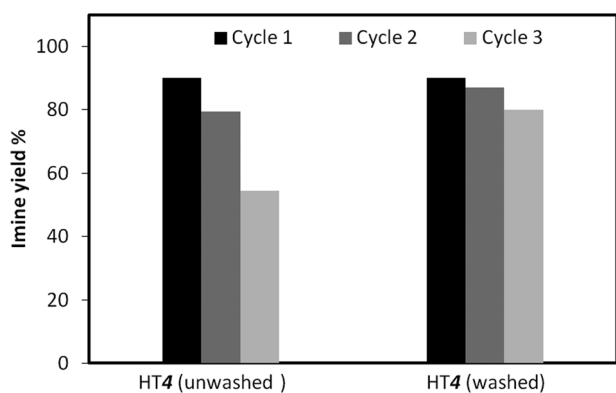


**Fig. 5** Percent yields of 4-methoxy-N-(phenylmethylene)benzenamine from repeated cycles of the alcohol imination reaction between benzyl alcohol and *p*-anisidine catalyzed by HT4.

nated after the aqueous  $K_2CO_3$  wash. The PXRD patterns and FT-IR spectra of the washed catalyst closely resemble those of the fresh catalyst.

Given these results, it was thus not surprising that as long as an aqueous  $K_2CO_3$  wash is performed, the catalyst retains its activity for at least 3 cycles with minimal loss in activity

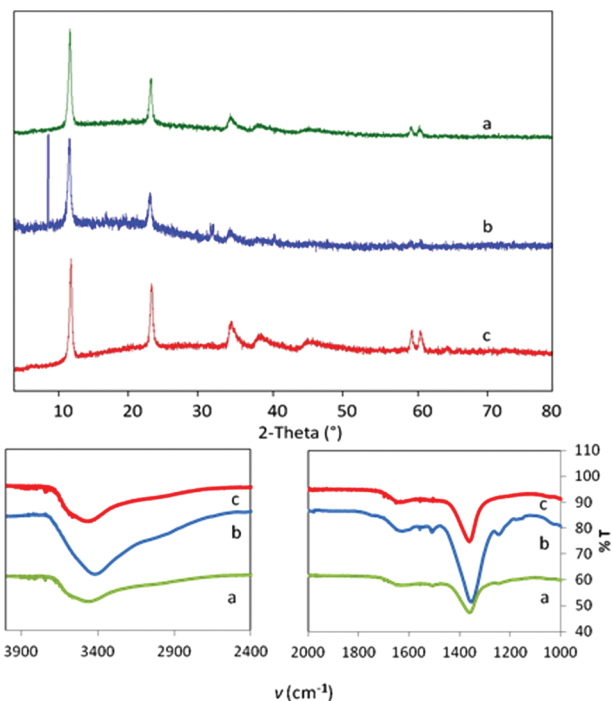


**Fig. 6** Powder X-ray diffraction patterns (above) and FT-IR spectra (below) of (a) HT4 washed with  $K_2CO_3$  (aq.) after an imination reaction, (b) HT4 – used and unwashed and (c) fresh HT4.

(Fig. 5). In contrast, the unwashed catalyst shows loss of catalytic activity quickly over 3 cycles (Fig. 5).

## Conclusions

We developed an active hydrotalcite-like (HT) heterogeneous catalyst for alcohol imination proceeding through acceptorless alcohol dehydrogenation. After screening HTs with different compositions (up to 15% of  $Fe^{3+}$ ,  $Zn^{2+}$ ,  $Ni^{2+}$ ,  $Cr^{3+}$  or  $Cu^{2+}$ ), we identified Fe:Mg:Al HT (HT4) as the most active for both dehydrogenation and imination. The yields of imine generally exceeded those of aldehydes, suggesting that the amine drives the equilibrium forward by condensation. Calcination slightly increased the activity for dehydrogenation but significantly lowered the activity for imination. Thus, we opted to enhance the catalytic activity of non-calcined HT4 by impregnating with  $Pd^0$  at 0.02%, ~1% and ~5% loading. The dehydrogenation activity of the catalysts was enhanced by  $Pd(0)$  immobilization, with 1%  $Pd/HT4$  affording the highest yield of aldehyde. However, the imination activity was reduced in a loading-dependent manner. Our experiments suggest that the primary reason for this was the  $Pd$  loading-dependent retention of aldehyde and imine on the catalysts. Substrate scope investigations revealed that the catalytic system is selective towards activated alcohols and aromatic amines. Recyclability experiments showed that the catalytic activity for imination can be retained for at least three cycles when HT4 is washed in aqueous  $K_2CO_3$ .

## Experimental

### Synthesis of HTs

Magnesium–aluminium hydrotalcites containing 0–15% Fe<sup>3+</sup>, Zn<sup>2+</sup>, Ni<sup>2+</sup>, Cr<sup>3+</sup>, and Cu<sup>2+</sup> were synthesized by aqueous co-precipitation of M<sup>2+</sup> and M<sup>3+</sup> nitrate salts under basic conditions (pH 8–10) in the presence of sodium carbonate (see Scheme 4 and ESI† for details).<sup>24</sup> The precipitates were filtered and washed copiously with deionized water until no more nitrate was present in the filtrate. The resulting hydrotalcites were dried at 110 °C for 12 hours, and a fraction of each sample was calcined at 450 °C for 24 h.

### Pd<sup>0</sup> supported on hydrotalcites

A series of Pd<sup>0</sup>/HT4 catalysts were prepared by wet precipitation–reduction. In a typical reaction, 2.00 g of calcined HT was suspended in deionized water (50 mL). To this suspension a known quantity of PdCl<sub>2</sub> was added, followed by the addition of 1 mL of a 1 M NaOH solution. The solution was allowed to stir at room temperature for 12 hours, after which the solution was removed *via* vacuum filtration, and the solid was washed with deionized water (3 × 25 mL) and dried for 12 hours at 110 °C. The solid was then resuspended in deionized water (50 mL) and reduced by dropwise addition of a NaBH<sub>4</sub> solution (0.01 g, 3 equivalents dissolved in 25 mL distilled water). The suspension was allowed to stir at room temperature for 2 hours, and then the solid was filtered and washed with deionized water (3 × 15 mL) and dried for 12 hours at 100 °C. Catalyst characterization is described in the ESI.†

### Alcohol dehydrogenation reactions

In a typical procedure, a 20 mL reaction tube was charged with 0.100 g of catalyst (or other amounts, as indicated). It was then evacuated and placed under a nitrogen atmosphere. Subsequently, the alcohol (0.24 mmol, 1 equiv.) and 3 mL of degassed solvent were added to the reaction tube. The reaction mixture was heated to 110 °C for 24 hours in a Heidolph Radleys Carousel 12 Plus Reaction Station. The reaction was filtered and the spent catalyst was washed with toluene (3 × 5 mL) and K<sub>2</sub>CO<sub>3</sub> (aq.) (3 × 5 mL). The filtrate was dried *in vacuo*, and the product was isolated by column chromatography using 80:20 hexanes–ethyl acetate. The isolated product was characterized by GC-MS, GC-FID and <sup>1</sup>H NMR.

### Alcohol imination reactions

In a typical procedure, a 20 mL reaction tube was charged with 0.100 g of catalyst (or other amounts, as indicated), then evacuated and placed under a nitrogen atmosphere. Subsequently the alcohol (0.24 mmol, 1 equiv.), amine (0.29 mmol, 1.2

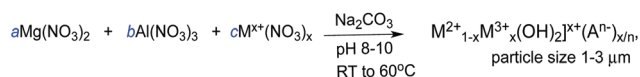
equiv.) and 3 mL of degassed solvent were added. The reaction mixture was heated to 110 °C for 24 hours in a Heidolph Radleys Carousel 12 Plus Reaction Station. The reaction was filtered and the spent catalyst was washed with toluene (3 × 5 mL) and K<sub>2</sub>CO<sub>3</sub> (aq.) (3 × 5 mL). The filtrate was dried *in vacuo*, and the product was isolated by column chromatography. The product was characterized by GC-MS and <sup>1</sup>H NMR.

## Acknowledgements

The authors would like to thank both Dr Chris Cahill and Dr Michael Wagner for the use of PXRD and BET measurements. The authors would also like to thank Dr Anastas Popratiľo and the Center for Microscopy and Image Analysis (CMIA) for providing training and access to the TEM.

## Notes and references

- 1 S. I. Murahashi, *Angew. Chem., Int. Ed. Engl.*, 1995, **34**, 2443–2465.
- 2 M. A. Berliner, S. P. A. Dubant, T. Makowski, K. Ng, B. Sitter, C. Wager and Y. S. Zhang, *Org. Process Res. Dev.*, 2011, **15**, 1052–1062.
- 3 J. F. Moulder, W. F. Stickel, P. E. Sobol and K. D. Bomben, *Handbook of X-ray Photoelectron Spectroscopy*, Physical-Electronics Inc., Eden Prairie, MN, 1995.
- 4 R. Kawahara, K. Fujita and R. Yamaguchi, *Adv. Synth. Catal.*, 2011, **353**, 1161–1168.
- 5 R. Yamaguchi, S. Kawagoe, C. Asai and K. I. Fujita, *Org. Lett.*, 2008, **10**, 181–184.
- 6 K. Fujita, Z. Z. Li, N. Ozeki and R. Yamaguchi, *Tetrahedron Lett.*, 2003, **44**, 2687–2690.
- 7 M. Benitez, E. Mas-Marza, J. A. Mata and E. Peris, *Chem. – Eur. J.*, 2011, **17**, 10453–10461.
- 8 G. E. Dobereiner and R. H. Crabtree, *Chem. Rev.*, 2010, **110**, 681–703.
- 9 K. Fujita, Z. Li, N. Ozeki and R. Yamaguchi, *Tetrahedron Lett.*, 2003, **44**.
- 10 D. Pinggen, C. Muller and D. Vogt, *Angew. Chem., Int. Ed.*, 2010, **49**, 8130–8133.
- 11 B. Gnanaprakasam, J. Zhang and D. Milstein, *Angew. Chem., Int. Ed.*, 2010, **49**, 1468–1471.
- 12 M. Hamid, C. L. Allen, G. W. Lamb, A. C. Maxwell, H. C. Maytum, A. J. A. Watson and J. M. J. Williams, *J. Am. Chem. Soc.*, 2009, **131**, 1766–1774.
- 13 N. Andrushko, V. Andrushko, P. Roose, K. Moonen and A. Borner, *ChemCatChem*, 2010, **2**, 640–643.
- 14 A. P. da Costa, M. Viciano, M. Sanau, S. Merino, J. Tejada, E. Peris and B. Royo, *Organometallics*, 2008, **27**, 1305–1309.
- 15 D. Gnanamgari, E. L. O. Sauer, N. D. Schley, C. Butler, C. D. Incarvito and R. H. Crabtree, *Organometallics*, 2009, **28**, 321–325.
- 16 K. I. Fujita, Y. Enoki and R. Yamaguchi, *Tetrahedron*, 2008, **64**, 1943–1954.



Scheme 4 Co-precipitation synthesis of hydrotalcites.

- 17 Y. Z. Qiang Kang, *Green Chem.*, 2012, **14**, 1016–1019.
- 18 G. Guillena, D. J. Ramon and M. Yus, *Chem. Rev.*, 2010, **110**, 1611–1641.
- 19 J. Xu, R. Zhuang, L. Bao, G. Tang and Y. Zhao, *Green Chem.*, 2012, **14**, 2384–2387.
- 20 E. L. Zhang, H. W. Tian, S. D. Xu, X. C. Yu and Q. Xu, *Org. Lett.*, 2013, **15**, 2704–2707.
- 21 G. Q. Zhang and S. K. Hanson, *Org. Lett.*, 2013, **15**, 650–653.
- 22 Y. Nakajima, Y. Okamoto, Y. H. Chang and F. Ozawa, *Organometallics*, 2013, **32**, 2918–2925.
- 23 S. Musa, S. Fronton, L. Vaccaro and D. Gelman, *Organometallics*, 2013, **32**, 3069–3073.
- 24 F. Cavani, F. Trifiro and A. Vaccari, *Catal. Today*, 1991, **11**, 173–301.
- 25 D. Meloni, M. F. Sini, M. G. Cutrufello, R. Monaci, E. Rombi and I. Ferino, *J. Therm. Anal. Calorim.*, 2012, **108**, 783–791.
- 26 V. R. L. Constantino and T. J. Pinnavaia, *Inorg. Chem.*, 1995, **34**, 883–892.
- 27 J. Kostal, A. Voutchkova-Kostal, B. Weeks, J. B. Zimmerman and P. T. Anastas, *Chem. Res. Toxicol.*, 2012, **25**, 2780–2787.
- 28 A. Vaccari, *Appl. Clay Sci.*, 1999, **14**, 161–198.
- 29 J. S. Valente, F. Figueras, M. Gravelle, P. Kumbhar, J. López and J. P. Besse, *J. Catal.*, 2000, **189**, 370.
- 30 S. Velu and C. S. Swamy, *Appl. Catal., A*, 1997, **162**, 81–91.
- 31 L. Dussault, J. C. Dupin, E. Dumitriu, A. Auroux and C. Guimon, *Thermochim. Acta*, 2005, **434**, 93–99.
- 32 S. Casenave, H. Martinez, C. Guimon, A. Auroux, V. Hulea, A. Cordoneanu and E. Dumitriu, *Thermochim. Acta*, 2001, **379**, 85–93.
- 33 J. S. Valente, F. Figueras, M. Gravelle, P. Kumbhar, J. Lopez and J. P. Besse, *J. Catal.*, 2000, **189**, 370–381.
- 34 M. R. Othman, Z. Helwani, Martunus and W. J. N. Fernando, *Appl. Organomet. Chem.*, 2009, **23**, 335–346.
- 35 S. K. Yun and T. J. Pinnavaia, *Chem. Mater.*, 1995, **7**, 348–354.
- 36 S. K. Sharma, P. K. Kushwaha, V. K. Srivastava, S. D. Bhatt and R. V. Jasra, *Ind. Eng. Chem. Res.*, 2007, **46**, 4856–4865.
- 37 D. G. Evans and D. A. Xue, *Chem. Commun.*, 2006, 485–496.
- 38 G. Fan, F. Li, D. G. Evans and X. Duan, *Chem. Soc. Rev.*, 2014, **43**, 7040–7060.
- 39 S. Nishimura, A. Takagaki and K. Ebitani, *Green Chem.*, 2013, **15**, 2026–2042.
- 40 J. Perez-Ramirez, S. Abello and N. M. van der Pers, *Chem. – Eur. J.*, 2007, **13**, 870–878.
- 41 K. K. Rao, M. Gravelle, J. S. Valente and F. Figueras, *J. Catal.*, 1998, **173**, 115–121.
- 42 D. P. Debecker, E. M. Gaigneaux and G. Busca, *Chem. – Eur. J.*, 2009, **15**, 3920–3935.
- 43 S. Abello, F. Medina, D. Tichit, J. Perez-Ramirez, J. C. Groen, J. E. Sueiras, P. Salagre and Y. Cesteros, *Chem. – Eur. J.*, 2005, **11**, 728–739.
- 44 M. J. Climent, A. Corma, S. Iborra and A. Velty, *J. Catal.*, 2004, **221**, 474–482.
- 45 A. R. Massah, R. J. Kalabashi, M. Toghiani, B. Hojati and M. Adibnejad, *E-J. Chem.*, 2012, **9**, 2501–2508.
- 46 O. D. Pavel, B. Cojocaru, E. Angelescu and V. I. Parvulescu, *Appl. Catal., A*, 2011, **403**, 83–90.
- 47 D. G. Cantrell, L. J. Gillie, A. F. Lee and K. Wilson, *Appl. Catal., A*, 2005, **287**, 183–190.
- 48 V. H. Jadhav, D. K. Dumbre, V. B. Phapale, H. B. Borate and R. D. Wakharkar, *Catal. Commun.*, 2007, **8**, 65–68.
- 49 T. Baskaran, R. Kumaravel, J. Christopher and A. Sakthivel, *RSC Adv.*, 2014, **4**, 11188–11196.
- 50 B. M. Choudary, M. L. Kantam, A. Rahman, C. V. Reddy and K. K. Rao, *Angew. Chem., Int. Ed.*, 2001, **40**, 763–766.
- 51 K. Takehira and T. Shishido, *Catal. Surv. Asia*, 2007, **11**, 1–30.
- 52 V. K. Diez, C. R. Apesteguia and J. I. Di Cosimo, *J. Catal.*, 2003, **215**, 220–233.
- 53 P. R. Likhari, R. Arundhathi, M. L. Kantam and P. S. Prathima, *Eur. J. Org. Chem.*, 2009, 5383–5389.
- 54 K. Motokura, N. Hashimoto, T. Hara, T. Mitsudome, T. Mizugaki, K. Jitsukawa and K. Kaneda, *Green Chem.*, 2011, **13**, 2416–2422.
- 55 S. Sueoka, T. Mitsudome, T. Mizugaki, K. Jitsukawa and K. Kaneda, *Chem. Commun.*, 2010, **46**, 8243–8245.
- 56 K. Motokura, D. Nishimura, K. Mori, T. Mizugaki, K. Ebitani and K. Kaneda, *J. Am. Chem. Soc.*, 2004, **126**, 5662–5663.
- 57 B. M. Choudary, S. Madhi, N. S. Chowdari, M. L. Kantam and B. Sreedhar, *J. Am. Chem. Soc.*, 2002, **124**, 14127–14136.
- 58 W. H. Fang, Q. H. Zhang, J. Chen, W. P. Deng and Y. Wang, *Chem. Commun.*, 2010, **46**, 1547–1549.
- 59 T. Mitsudome, Y. Mikami, K. Ebata, T. Mizugaki, K. Jitsukawa and K. Kaneda, *Chem. Commun.*, 2008, 4804–4806.
- 60 T. Mitsudome, Y. Mikami, H. Funai, T. Mizugaki, K. Jitsukawa and K. Kaneda, *Angew. Chem., Int. Ed.*, 2008, **47**, 138–141.
- 61 K. Kaneda, T. Mitsudome, T. Mizugaki and K. Jitsukawa, *Molecules*, 2010, **15**, 8988–9007.
- 62 K. Takehira, T. Shishido, P. Wang, T. Kosaka and K. Takaki, *Phys. Chem. Chem. Phys.*, 2003, **5**, 3801–3810.
- 63 J. Chen, Q. H. Zhang, W. H. Fang, Y. Wang and H. L. Wan, *Chinese J. Catal.*, 2010, **31**, 1061–1070.
- 64 W. H. Fang, J. S. Chen, Q. H. Zhang, W. P. Deng and Y. Wang, *Chem. – Eur. J.*, 2011, **17**, 1247–1256.
- 65 R. K. Marella, C. K. P. Neeli, S. R. R. Kamaraju and D. R. Burri, *Catal. Sci. Technol.*, 2012, **2**, 1833–1838.
- 66 R. J. Shi, F. Wang, X. L. Mu, N. Ta, Y. Li, X. M. Huang and W. J. Shen, *Chin. J. Catal.*, 2010, **31**, 626–630.
- 67 N. Kakiuchi, Y. Maeda, T. Nishimura and S. Uemura, *J. Org. Chem.*, 2001, **66**, 6620–6625.
- 68 T. Nishimura, N. Kakiuchi, M. Inoue and S. Uemura, *Chem. Commun.*, 2000, 1245–1246.
- 69 R. Jenkins and R. L. Snyder, *Introduction to X-ray Powder Diffractometry*, John Wiley & Sons Inc., 1996.
- 70 S. Velu, V. Ramkumar, A. Narayanan and C. S. Swamy, *J. Mater. Sci.*, 1997, **32**, 957–964.
- 71 T. Chen, F. Z. Zhang and Y. Zhu, *Catal. Lett.*, 2013, **143**, 206–218.

- 72 J. T. Feng, X. Y. Ma, Y. F. He, D. G. Evans and D. Q. Li, *Appl. Catal., A*, 2012, **413**, 10–20.
- 73 S. Narayanan and K. Krishna, *Appl. Catal., A*, 1998, **174**, 221–229.
- 74 D. E. Ramaker, J. de Graaf, J. A. R. van Veen and D. C. Koningsberger, *J. Catal.*, 2001, **203**, 7–17.
- 75 N. Kakiuchi, T. Nishimura, M. Inoue and S. Uemura, *Bull. Chem. Soc. Jpn.*, 2001, **74**, 165–172.
- 76 M. Granollers, R. Brown, N. An, P. Yaseneva, A. P. Voutchkova-Kostal and A. Lapkin, Microcalorimetric studies of doped hydrotalcite-like materials: effect of synthetic conditions. Manuscript in preparation.